Int J Adv Manuf Technol (2018) 98:189–200
https://doi.org/10.1007/s00170-017-1228-7

ORIGINAL ARTICLE

Rotary ultrasonic drilling of needle-punched carbon/carbon composites: comparisons with conventional twist drilling and high-speed drilling

Chenwei Shan[1] · **Xu Zhang**[1] · **Jie Dang**[1] · **Yang Yang**[1]

Received: 14 December 2016 / Accepted: 17 October 2017 / Published online: 10 November 2017

Abstract Drilling of carbon/carbon (C/C) composites is difficult to carry out due to its high specific stiffness, brittleness, anisotropic, non-homogeneous, and low thermal conductivity, which can result in tear, burr, poor surface quality, and rapid wear of tools. Three drilling methods including conventional twist drilling, rotary ultrasonic drilling, and high-speed drilling can all be used in hole making of composites in industry. To find a best method of hole making in drilling of C/C composites, a serials of comparison experimental tests using the same size cemented carbide drill are designed and performed in this paper. Thrust force, tool wear, and drilling defects are all analyzed and compared for different machining parameters for all the three drilling methods. The experimental results show that rotary ultrasonic drilling is the best choice in almost all these aspects in drilling of needle-punched C/C composites within the range of selected experimental machining parameters.

Keywords Carbon/carbon composites · Conventional twist drilling · Rotary ultrasonic drilling · Drilling force · Drilling defects

1 Introduction

C/C composites are carbon fiber-reinforced carbon matrix composites. They are the new ultra-high-temperature structural material possessing many outstanding performances, such as high heat resistance, along with lightweight, high resistance to corrosion, high stiffness, and high strength [1]. C/C composites can retain room temperature properties to more than 3000 °C in the inert atmosphere; this is the main trend of the development of high-temperature structural materials in the future [2]. Due to these special characteristics, C/C composites lend itself well to aerospace field, such as aircraft braking systems and solid rocket nozzle.

Conventional machining operations of C/C composites, such as turning, milling, and drilling, which are a problem as the fibers and fiber direction result in an uneven cutting force and high tool wear, can still be applied to the machining of C/C composites. Drilling operations are often required before mechanical joining of the C/C composites components. Conventional twist drilling (CTD) is a fast and effective hole-making method for secondary machining of composite structures. Due to the economic reasons, the two-lip conventional twist drill (used for the drilling of metallic materials) is employed to drill composite structures [3]. However, some characteristics of C/C composites such as high specific stiffness, brittleness, anisotropic, and non-homogeneous and low thermal conductivity, make it difficult to machine. The most frequent drilling-induced defects are tear, burr, delamination, and edge breakage in addition to other minor damages. To reduce or eliminate these defects in drilling of composite structures, many researchers are trying to optimize machining parameters and to find some better methods than CTD.

Because rotary ultrasonic drilling (RUD) is an excellent method in drilling of brittle materials, it has been used in drilling of composite structures in recent years by some researchers [4–8]. RUD is a kind of periodic pulse cutting instead of continuous cutting. Compared

✉ Chenwei Shan
shancw@nwpu.edu.cn

[1] Key Laboratory of Contemporary Design and Integrated Manufacturing Technology, Ministry of Education, Northwestern Polytechnical University, Xi'an 710072, China

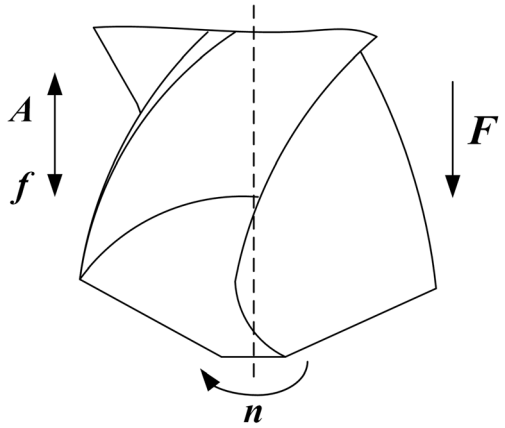

Fig. 1 Schematic diagram of the two-lip twist drill

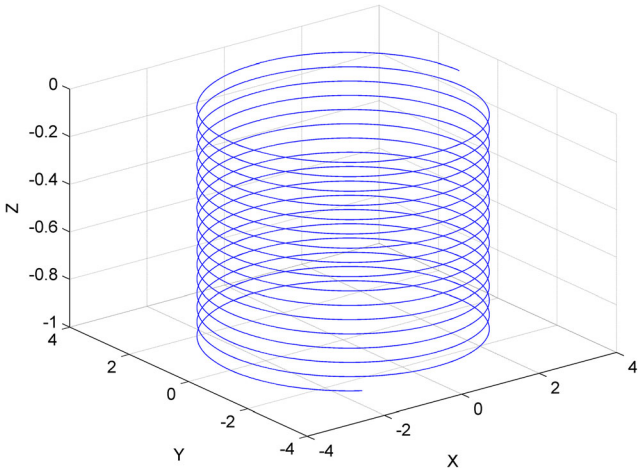

Fig. 3 Motion trajectory of the point P in CTD (F = 60 mmpm, n = 1000 rpm, D = 6 mm)

with conventional drilling, it can effectively reduce the cutting force and temperature, and can obviously improve the hole quality and tool life. Li et al. [9] studied RUD on ceramic matrix composites and found that RUD has lower cutting force, better material removing rate than conventional drilling. Liu et al. [10] investigated the chipping and tool wear at the exit of the hole in RUD of ceramic materials and found that low feed rate, adequate amount of axial vibration, and high cutting speed as optimal parameters are suitable for hole making. Ning et al. [11] established a mechanistic calculation model in RUD of carbon fiber-reinforced polymer composites (CFRP) and provided a relationship between amplitude of ultrasonic vibration and different input variables. Cong et al. [12, 13] found that rotary ultrasonic machining (RUM) can obviously reduce cutting force, delamination, and surface roughness by experimental methods in drilling of CFRP, and then established a theoretical model to predict the cutting force of RUD of CFRP. Liu et al. [14] found that the rotary ultrasonic elliptical machining (RUEM) using core drill could reduce the average cutting force and torque significantly in drilling CFRP. In RUD of composites, most researchers focus on drilling of CFRP or ceramic matrix composites. However, there are few literatures focusing on drilling technology of C/C composites.

High-speed drilling (HSD) plays an important role in increasing productivity as well as material removal rate and thus, decreasing machining cost [15, 16]. Hence, some researchers have done many works on drilling of composite structures by using HSD. Karnik et al. [17] developed an artificial neural network model with spindle speed, feed rate, and point angle as the affecting parameters to analyze the effects of drilling process parameters on delamination factor, which demonstrated the advantage of employing higher speed in controlling the delamination during drilling. Campos Rubio et al. [18] employed HSD in drilling of glass fiber-reinforced plastics (GFRP) to improve the performance, and presented an adjusted delamination factor to assess delamination. The results indicated that HSD is suitable for drilling GFRP ensuring low damage levels. Lin and Chen [19] studied the effects of HSD on average thrust force, torque, drill wear, and hole quality for both multifaceted drill and twist drill on CFRP materials, and found that increasing cutting speed will accelerate tool wear, and tool wear is the major problem encountered when drilling CFRP at high speed within the range of cutting speed examined. Gaitonde et al. [20] presented an investigative analysis of parametric influence

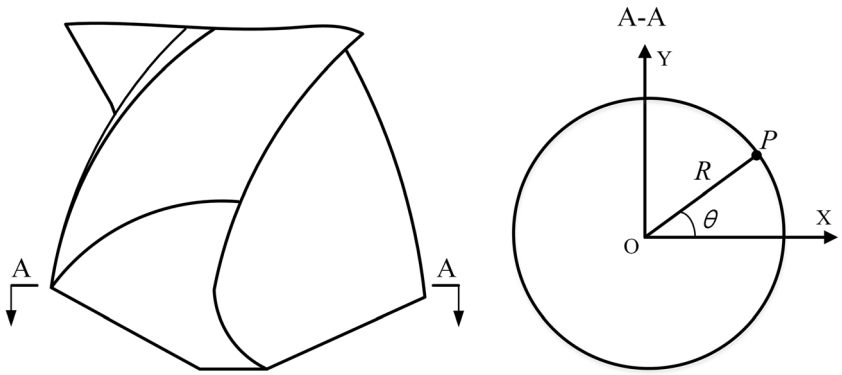

Fig. 2 Circumscribed circle of the cross section of twist drill

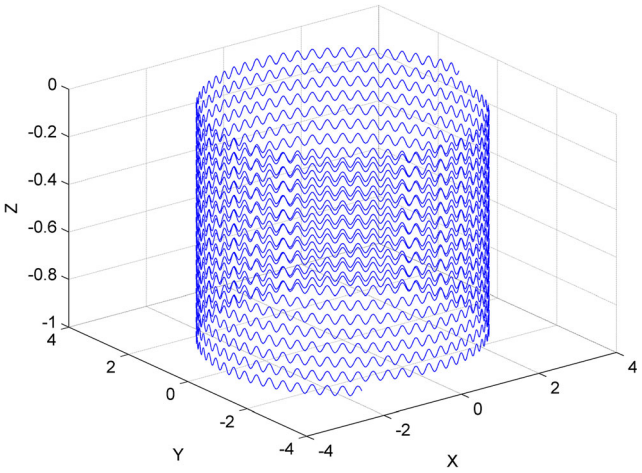

Fig. 4 Motion trajectory of the point P in RUD (f = 1000 Hz, A = 20 μm, F = 60mmpm, n = 1000 rpm, D = 6 mm)

on delamination factor in HSD of CFRP, and the results indicated that the combination of low feed rate and point angle is also essential in minimizing delamination during drilling of CFRP composites. Krishnaraj et al. [21] studied the effect of cutting parameters such as spindle speed and feed rate in HSD of thin CFRP laminates using K20 carbide drill by an experimental test of a full factorial design. Genetic algorithm methodology was used to find the optimum cutting conditions for defect-free drilling, and the optimized spindle speed and feed rate for drilling thin CFRP laminates at high speeds were found to be 12,000 rpm and 0.137 mm/rev, respectively.

To find a good method in drilling of C/C composites, a serials of experimental tests including CTD, RUD and HSD using the same size cemented carbide drill are carried out and compared with each other. Four types of feed speed are tested for different spindle speeds by using a single factorial design. Thrust force, tool wear, and drilling defects are all analyzed and compared for CTD, RUD, and HSD.

2 Motion trajectory of drill in RUD

The two-dimensional model of the two-lip twist drill used in RUD is schematically illustrated in Fig. 1, where f and A are the frequency and amplitude of ultrasonic vibration applied to the twist drill, respectively. F is the feed speed in millimeters per minute, n is the spindle speed in revolutions per minute.

It can be seen from Fig. 1 that the ultrasonic vibration is applied only in the axial direction, the axial displacement of the twist drill due to axial vibration can be expressed as follows:

$$z_1(t) = A\sin(2\pi ft) \tag{1}$$

where t is the time in second.

And the axial displacement of the twist drill due to feed speed can be expressed as follows:

$$z_2(t) = \frac{Ft}{60} \tag{2}$$

Then, the total axial displacement of the twist drill in RUD can be obtained as follows:

$$z_{\mathrm{RUD}}(t) = z_1(t) + z_2(t) = A\sin(2\pi ft) + \frac{Ft}{60} \tag{3}$$

As shown in Fig. 2, the circle on the right is the circumscribed circle of the cross section of the two-lip twist drill on the left. And the point P represents a point on the circle, assuming that the diameter of the twist drill is D, then R is half of D. θ is the rotation angle with respect to X-axis.

The relationship between the rotation angle θ of the twist drill and time t in drilling can be expressed as follows:

$$\theta(t) = \frac{2\pi nt}{60} = \frac{\pi nt}{30} \tag{4}$$

Assuming that the feed direction is negative Z-axis, then at any time t, the motion trajectory of the point P in CTD and

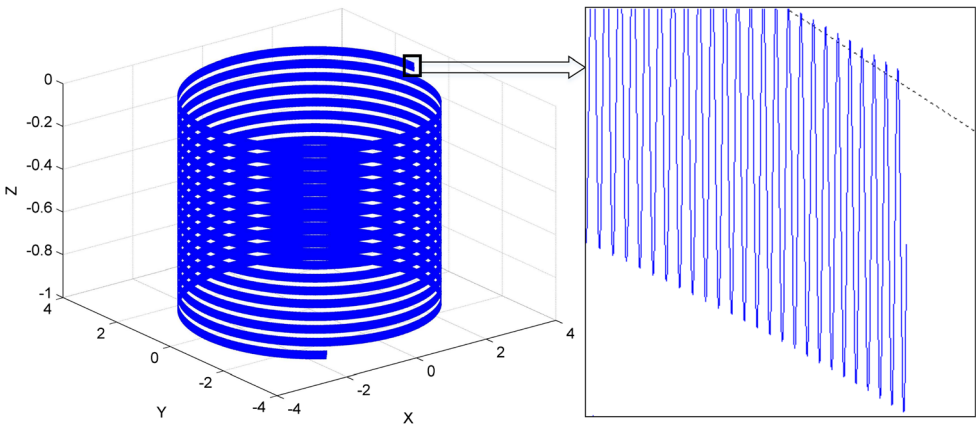

Fig. 5 Motion trajectory of the point P in RUD (f = 20 KHz, A = 20 μm, F = 60 mmpm, n = 1000 rpm, D = 6 mm)

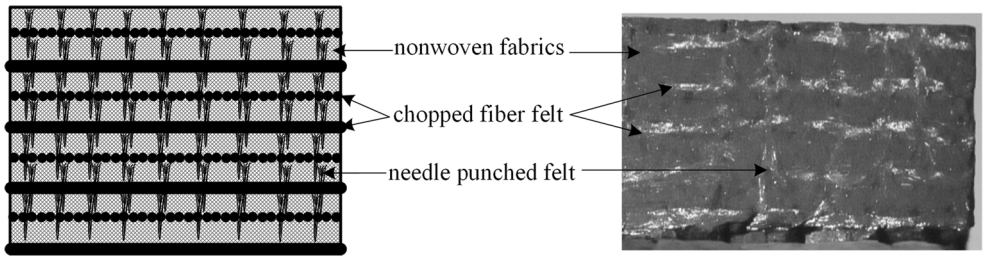

Fig. 6 Structure figure of C/C composites [22]

RUD, that is the outline of the motion trajectory of the twist drill, can be respectively expressed as follows:

$$\begin{cases} x_{\mathrm{CTD}}(t) = \dfrac{D}{2}\cos(\pi nt/30) \\ y_{\mathrm{CTD}}(t) = \dfrac{D}{2}\sin(\pi nt/30) \\ z_{\mathrm{CTD}}(t) = -\dfrac{Ft}{60} \end{cases} \tag{5}$$

$$\begin{cases} x_{\mathrm{RUD}}(t) = \dfrac{D}{2}\cos(\pi nt/30) \\ y_{\mathrm{RUD}}(t) = \dfrac{D}{2}\sin(\pi nt/30) \\ z_{\mathrm{RUD}}(t) = -A\sin(2\pi ft) - \dfrac{Ft}{60} \end{cases} \tag{6}$$

The input parameters used in the subsequent experiment of CTD are set as follows: F is 60 mmpm, n is 1000 rpm, and D is 6 mm, then the motion trajectory of point P in CTD can be obtained by calculating Eq. (5), as shown in Fig. 3. It can be seen from Fig. 3 that the motion trajectory of the point P in CTD is a spiral, and its axial spacing is constant.

Assuming that the frequency f and the amplitude A of ultrasonic vibration applied to the twist drill is 1000 Hz and 20 μm, and other input parameters are the same as CTD, then the motion trajectory of the point P in RUD can be obtained by calculating Eq. (6), as shown in Fig. 4. It can be seen from Fig. 4 that the axial displacement of the twist drill has a periodical change.

In general, the actual frequency of ultrasonic vibration exceeds 20 KHz. Hence, when the frequency is set as 20 KHz, and other input parameters also are the same as CTD, then as shown in Fig. 5, the motion trajectory of the point P in RUD, which is more close to reality, can be obtained. It can be seen from the left side of Fig. 5 that the motion trajectory of the point P in RUD becomes very denser due to the large frequency than before, and the periodical change of the axial displacement can also be observed from the enlarged picture on the right side of Fig. 5. The special characteristic of the motion trajectory can lead to the lower cutting force and temperature, and also the different cutting mechanism compared with CTD.

3 Experimental conditions

3.1 Workpiece material

The C/C composites workpiece used in this paper is produced by laminating the nonwoven fabrics and chopped carbon fiber felt one over another and subjecting the laminated nonwoven fabrics to needle punched repeatedly with a plurality of needles, thereby yielding a fabric body of three-dimensional structure and carbonizing obtained fabric body by chemical vapor infiltration (CVI) method with vaporized kerosene as a precursor. The microstructure of this C/C composite with needle-punched felt is shown in Fig.6. The mechanical properties of the material are shown in Table 1. Although this material is reinforced by needle-punched felt, it is strong in the fiber direction, quite weak in the needle-punched direction [22].

3.2 Tool

All the experiments of the three drilling methods are conducted by using cemented carbide (K40) twist drills. The parameters of the twist drills are shown in Table 2, and the twist drill is shown in Fig.7.

Table 1 Parameters and properties of the material

Material parameter	Direction	Value
Tensile strength (MPa)	Axial	58.9
	Radial	89.8
Compressive strength (MPa)	Axial	130
	Radial	212
Interlaminar shear strength (MPa)		14.2

Table 2 Parameters of the twist drills

Parameters	Unit	Value
Diameter	mm	6
Tool length	mm	90
Cutting length	mm	20
Point angle		118°
Helix angle		30°
Relief angle		14°

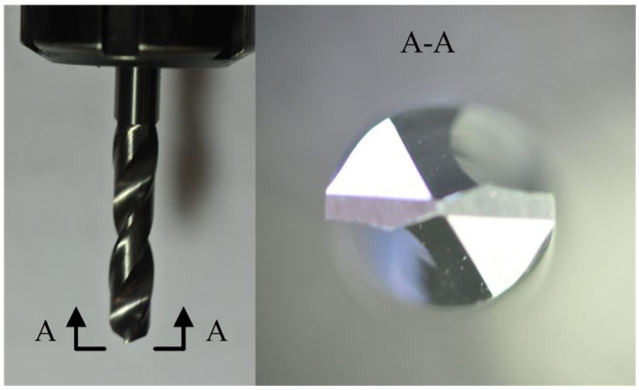

Fig. 7 Cemented carbide drill

Table 3 Parameters of the ultrasonic vibration device

Parameters	Unit	Value
Power	W	150
Frequency	KHz	20
Amplitude	μm	20

3.3 Experimental setup

The experiments are carried out in the JOHNFORD VMC850 four-axis machining center, equipped with a FANUC-OI-MB NC unit. The thrust force signals during drilling are measured using the Kistler dynamometer 9255B. Dynamometer is charged and the signals are collected by a data acquisition system which includes a Kistler multi-channel charge amplifier 5019B and Kistler DynoWare software.

The ultrasonic vibration system contained an ultrasonic vibration tool holder and an ultrasonic generator. The parameters of this ultrasonic vibration device are shown in Table 3. Because the function of the ultrasonic vibration device is limited, the frequency of ultrasonic vibration is fixed as 20 KHz and cannot be changed. Nevertheless, for the specific cutting tool used in the experiments, that is, in the case of the same load, the fixed frequency can make sure that the ultrasonic vibration system work well and the machining result is well. The ultrasonic vibration tool holder which is installed in the machine spindle is shown in Fig. 8, and the experimental setup of RUD is schematically illustrated in Fig.9. Because the maximum spindle speed of the machine is only 8000 rpm, a spindle speeder MV-7C made in Madaula company of Spain is adopted, and the speed increasing ratio is 1:7. The maximum speed of the spindle speeder is 25,000 rpm.

3.4 Experimental parameters

The same drilling parameters including spindle speed and feed speed are used both in RUD and CTD, as shown in Table 4. The same feed speeds used in RUD and CTD are also adopted in HSD. Four different actual spindle speeds are selected carefully for HSD according to the increasing ratio of the spindle speeder. The drilling parameters of HSD are shown in Table 5.

4 Experimental results

4.1 Drilling thrust force

4.1.1 Comparison of thrust force between RUD and CTD

To avoid the inaccuracy of single specimen, three holes are drilled for each drilling parameter selected in Tables 4 and 5, and all thrust forces are recorded by using the dynamometer. The average thrust force (F_z) of the three holes is calculated using the same drilling parameters in the drilling stable stage.

Table 6 shows the results of the average thrust force in RUD and CTD. It can been seen from Table 6 that thrust forces in RUD are much lower than that in CTD at all the same parameters. Obviously, RUD is helpful to reduce cutting forces. Within the range of drilling parameters selected, thrust forces in RUD are reduced by up to 41.9% maximally and 26.5%, averagely.

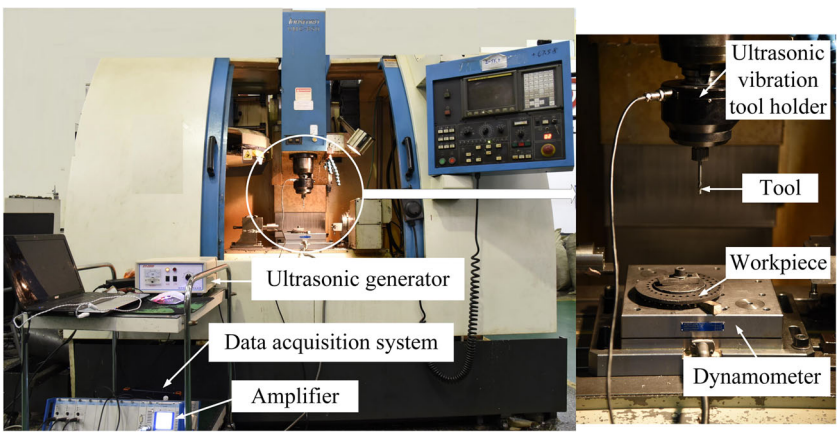

Fig. 8 Experimental setup of RUD

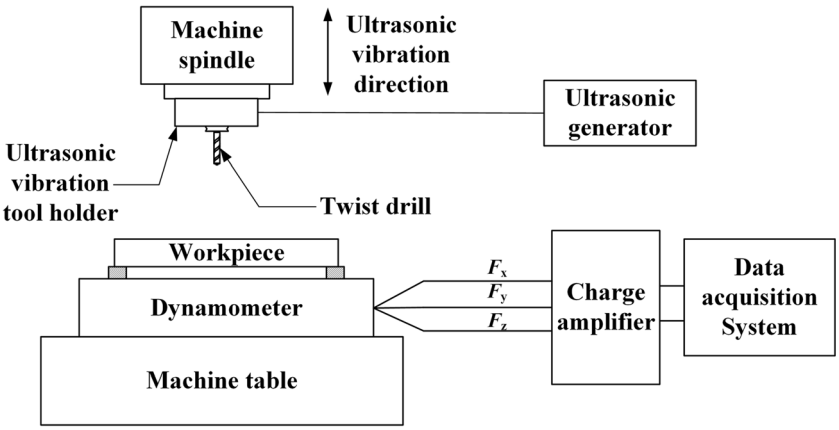

Fig. 9 Schematic diagram of the experimental setup of RUD

Furthermore, the reduction of thrust force is the maximum when the spindle speed increases to 5000 rpm. The main reason is that when the cutting speed becomes higher, the tool wear of CTD will become more serious than that of RUD, as a result, thrust forces will increase considerably.

Figure10 shows a comparison of thrust force between RUD and CTD when feed speed is changed from 60 to 150 mmpm. For both RUD and CTD, thrust forces increase with the increasing of feed speed. Thrust forces in RUD are much lower than that in CTD at the same feed speed and spindle speed. The increasing trend of thrust force in RUD becomes slow with the increasing of feed speed; however, the trend of CTD is more volatile.

Figure 11 shows a comparison of thrust force between RUD and CTD when spindle speed is changed from 1000 to 5000 rpm. For both RUD and CTD, thrust forces decrease as the spindle speed increases from 1000 to 4000 rpm. However, when the spindle speed exceeds 4000 rpm, thrust forces appear a rise trend with the increasing of spindle speed. Obviously, the cutting edge of the drill becomes blunt when the spindle speed is greater than 4000 rpm; this is owing to the fact that the uncoated drills will wear quickly with the increasing of the cutting speed.

4.1.2 Comparison of thrust force between RUD and HSD

Figure 12 shows a comparison of thrust force between RUD and HSD when feed speed is changed from 60 to 150 mmpm. Figure 13 shows the effect of spindle speed on thrust force in HSD when feed speed is changed from 7000 to 14,000 rpm.

For both RUD and HSD, the spindle speeds selected are all 1000 and 2000 rpm. Because the speed increasing ratio of the spindle speeder is 1:7, the actual spindle speeds in HSD are 7000 and 14,000 rpm.

Thrust forces in HSD are lower than that in RUD when the spindle speed in RUD is 1000 rpm and that in HSD is 7000 rpm. However, thrust forces in HSD are much higher than that in RUD when the spindle speed in RUD is 7000 rpm and that in HSD is 14,000 rpm. Furthermore, it can be seen from Fig. 13 that thrust forces in HSD show a slow downward trend when the spindle speed increases from 7000 to 9100 rpm. However, they present a rapid rise trend when the spindle speed increases from 9100 to 14,000 rpm. Hence, the high-speed cutting is of benefit to decrease thrust force when the spindle speed is less than 9100 rpm for the 6 mm diameter drill, that is, the cutting speed should be less than 24.49 m/min. When the cutting speed becomes larger than 24.49 m/min, the high-speed cutting will lead to high thrust forces because the drill may become blunt seriously under the high-temperature and high-speed impact.

Compared with CTD and HSD, RUD is a type of pulsed intermittent cutting process, thus cutting chips in RUD are removed timely and cutting resistant forces in RUD are lower than that in CTD and HSD. As a result, RUD can reduce thrust

Table 4 Experimental parameters of RUD and CTD

Parameters	Unit	Value
Spindle speed (n)	rpm	1000,2000,3000,4000,5000
Feed speed(F)	mmpm	60,90,120,150
Coolant style		Dry cutting

Table 5 Experimental parameters of HSD

Parameters	Unit	Value
Machine spindle speed (n)	rpm	1000,1300,1600,2000
Increasing ratio		1:7
Actual spindle speed (n)	rpm	7000,9100,11,200,14,000
Feed speed (F)	mmpm	60,90,120,150
Coolant style		Dry cutting

Table 6 Results of thrust force

No.	*n* (rpm)	*F* (mmpm)	Thrust force/*N*		Relative reduction (%)
			RUD/*N*	CTD/*N*	
1	1000	60	20.203	30.674	34.14
2	1000	90	25.321	36.453	30.54
3	1000	120	30.877	39.41	21.65
4	1000	150	33.127	45.493	27.18
5	2000	60	14.659	20.641	28.98
6	2000	90	19.982	25.085	20.34
7	2000	120	22.367	27.5	18.67
8	2000	150	25.625	32.544	21.26
9	3000	60	13.724	18.103	24.19
10	3000	90	17.017	21.869	22.19
11	3000	120	18.032	23.754	24.09
12	3000	150	19.168	28.235	32.11
13	4000	60	10.231	12.133	15.68
14	4000	90	11.576	15.698	26.26
15	4000	120	14.054	17.751	20.83
16	4000	150	15.812	19.321	18.16
17	5000	60	8.095	11.099	27.07
18	5000	90	12.225	19.984	38.83
19	5000	120	14.096	24.269	41.92
20	5000	150	17.332	27.086	36.01
The average reduction					26.5

forces and cutting temperature greatly, hence, the tool life can be improved.

4.2 Tool wear

The tool wear is measured by using the InfiniteFocus G4 tool measuring instrument produced by Alicona. The flank faces at the main cutting edge are enlarged 10 times to compare the tool wear of the three drilling methods.

Figure 14 shows the comparison of tool wear among RUD, CTD, and HSD. All of them are observed after drilling 12 holes. It can be seen that RUD can effectively reduce tool wear, and the tool wear in HSD was the most serious of all. Compared with RUD, the tool wear both in CTD and HSD are serious, this is mainly caused by the higher cutting temperature and cutting force in the drilling process. Because RUD can reduce thrust force more greatly than CTD and HSD at the same spindle speed and feed speed, the tool life in RUD is the longest of all.

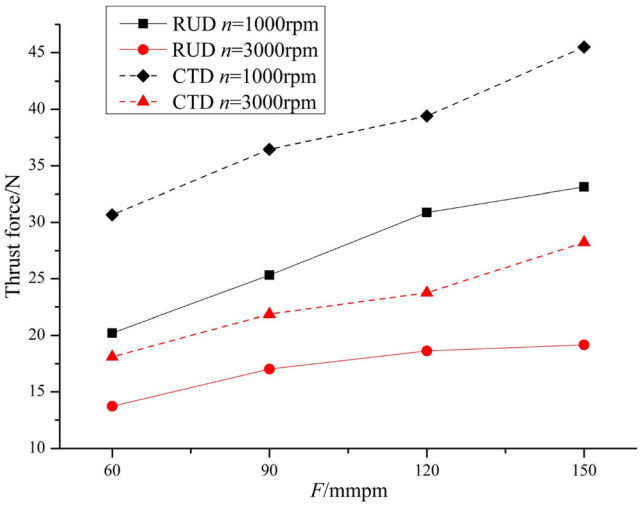

Fig. 10 Thrust force versus feed speed in RUD and CTD

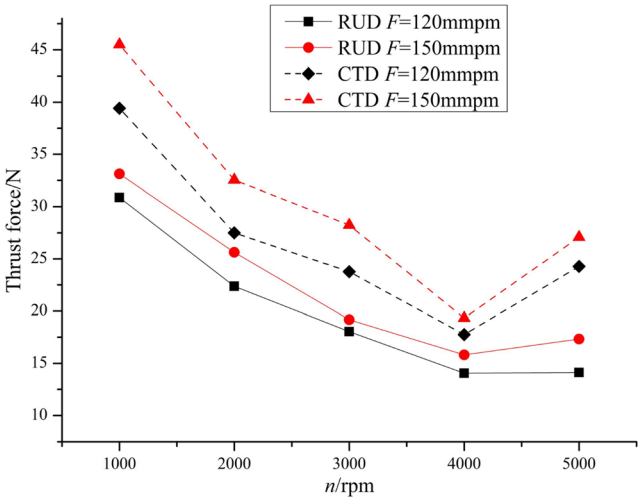

Fig. 11 Thrust force versus spindle speed in RUD and CTD

4.3 Drilling defects

There are three major types of defects at the exit of the holes in drilling of C/C composites, such as fiber burr, tear, and chipping. The chipping defect can be regarded as tiny tear. The defects of burr and tear are the most common defects in

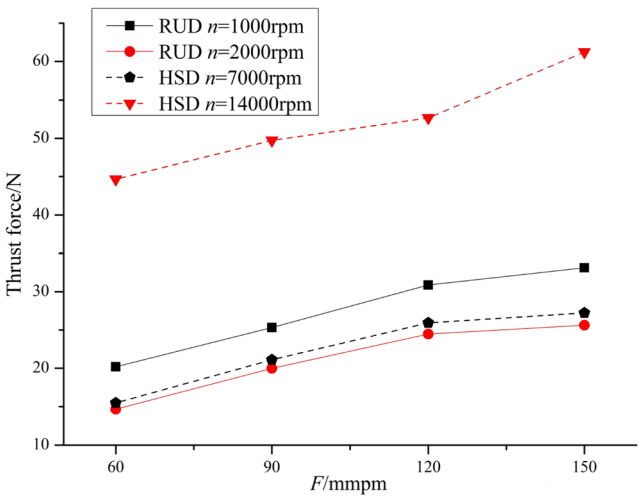

Fig. 12 Thrust force versus feed speed in RUD and HSD

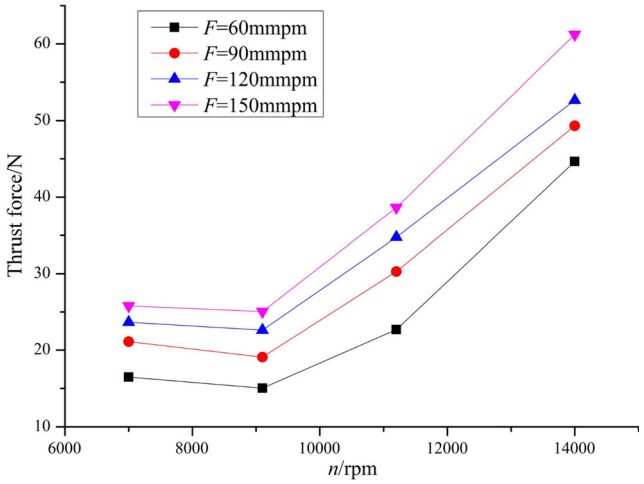

Fig. 13 Effect of spindle speed on thrust force in HSD

drilling of C/C composites. They are the important factors to evaluate the quality of holes, which have an important effect on the assembly quality of workpiece. The holes are enlarged 100 times for observing the defects under the microscope, and the drilling defects are compared among all the three different processing methods.

4.3.1 Burr defect

Generally, the outer surfaces of the specimen of 2.5D C/C composites may be nonwoven fabrics or chopped fiber felt. If the bottom surface of the specimen is nonwoven fabric layer, burr defects often appear at the exit of the holes.

In this paper, burr factor is used to evaluate the degree of burr; it can be calculated by using Eq. (7) presented in [23].

$$f_{burr} = \frac{4\alpha}{\pi d^2} \sum_{i=1}^{n} S_i + \frac{\beta}{\pi d} \sum_{i=1}^{n} l_i \tag{7}$$

where d is the nominal diameter of the hole, l_i is the length of the ith small burr, and S_i is the area of the ith large burr. Both α and β are weight, $\alpha + \beta = 1$. Because small burrs have little effect on the assembly, α is set as 0.9, and β is set as 0.1 in this paper.

Figs. 15 and 16 show the burr defects at the exit of the holes in RUD, CTD, and HSD, which are enlarged 100 times under the microscope. Figure 17 shows the burr factors of the three types of drilling methods when feed speed is changed from 60 to 150mmpm. It can be seen from Fig. 17 that the burrs in CTD are more serious than that in RUD. Although there are some improvements of decreasing burr defects in RUD, the effect is not obvious. The burr length in HSD is the smallest when the feed speed is less than 120mmpm. The reason is that the Z-direction tensile strength of 2.5D C/C composites is much lower than the X-direction and Y-direction, and it is difficult to cut off the fibers completely in RUD and CTD at a low cutting speed before the fibers lose bonding with matrix. In HSD, due to its high-speed cutting, it is conducive to cut off the fibers. However, the burr length in HSD will grow up when the feed speed is more than 120 mmpm because the cutting edge of drill will wear and become blunt quickly.

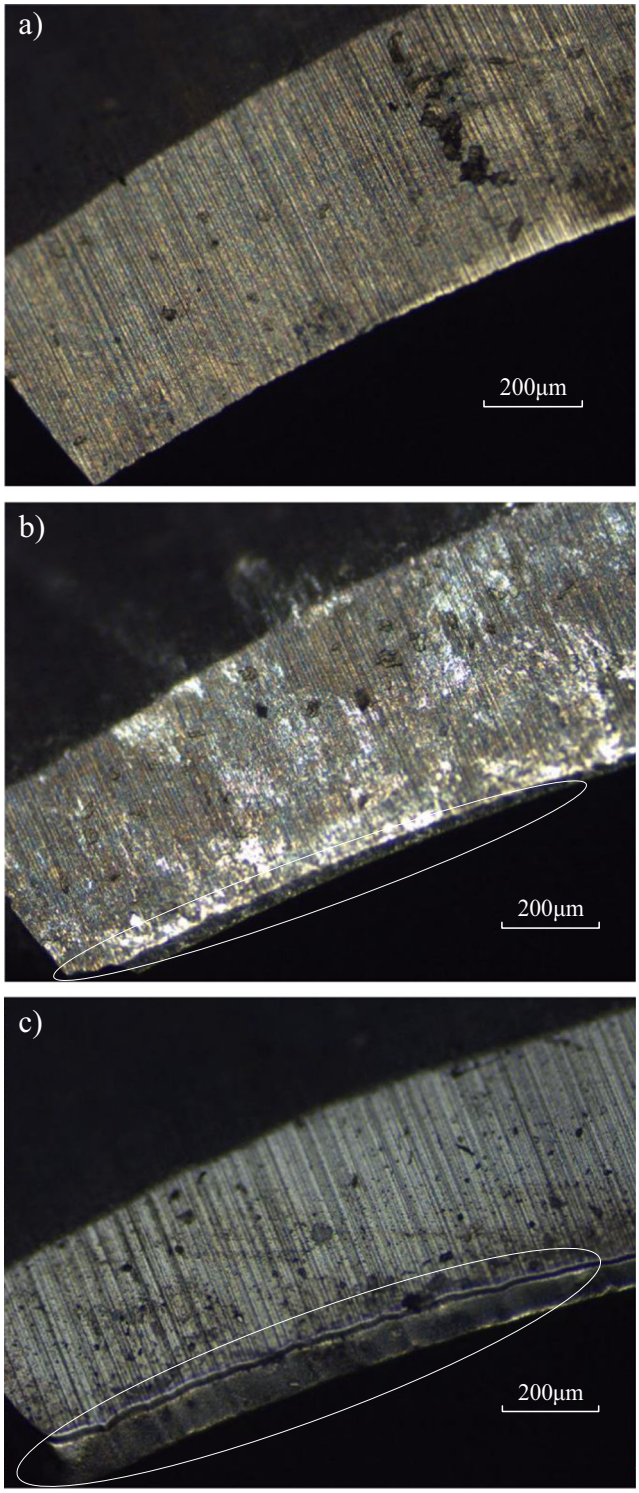

Fig. 14 Tool wear at the main cutting edge. **a** RUD. **b** CTD. **c** HSD

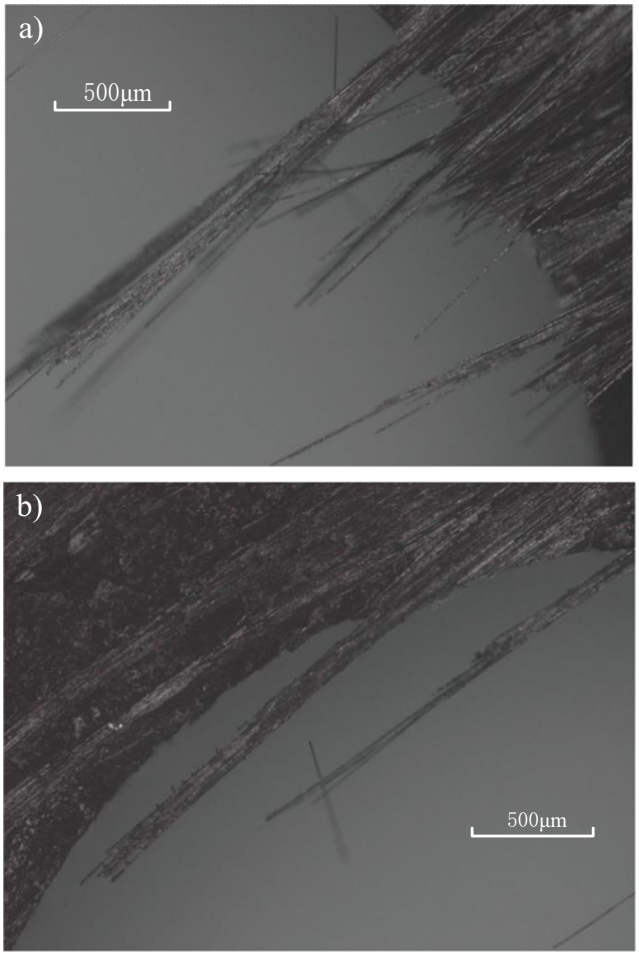

Fig. 15 Burr defects at the exit of the holes in RUD and CTD (n = 1000 rpm, F = 120 mmpm). **a** CTD. **b** RUD

4.3.2 Tear defect

According to the observation at the exit of the holes, when the exit layer is the chopped fiber felt layer, both burr defects and tear defects are not serious. However, when the exit layer is the nonwoven fabrics, both burr and tear defects become more serious.

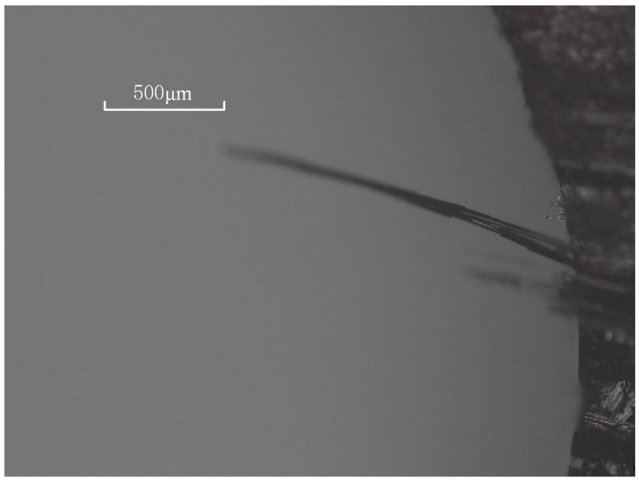

Fig. 16 Burr defects at the exit of the hole in HSD (n = 7000 rpm, F = 120 mmpm)

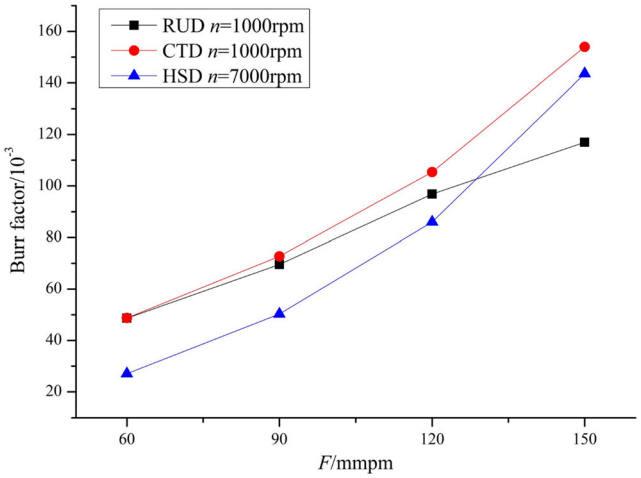

Fig. 17 Burr factors versus feed speed in RUD, CTD, and HSD

In this paper, tear factor is used to evaluate the degree of tear, it is described by D_t/D. As shown in Fig.18, D is the hole diameter. D_t is the largest circle that encloses all the tear area around the hole. According to the tear factor, the tear defect can be classified into three types. If the tear factor is less than 1.07, the defect is chipping; if it is more than 1.07 and less than 1.25, the defect is tear; if it is more than 1.25, the defect is delamination.

Figs. 19 and 20 show the tear defects in RUD, CTD, and HSD, which are enlarged 100 times under the microscope. Figs. 21, 22, and 23 show the tear factors in RUD, CTD, and HSD when drilling process parameters are changed. At all levels of feed speeds and spindle speeds, tear factors in RUD are the smallest in the three types drilling methods. Moreover, most of the tear factors in RUD are less than 1.07, which means chipping is the main defect in RUD.

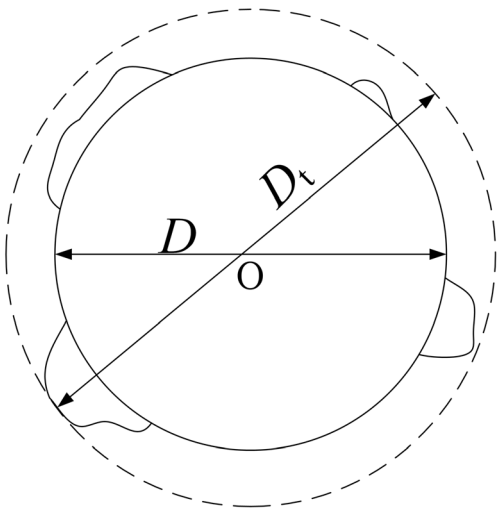

Fig. 18 Measurement of tear factor

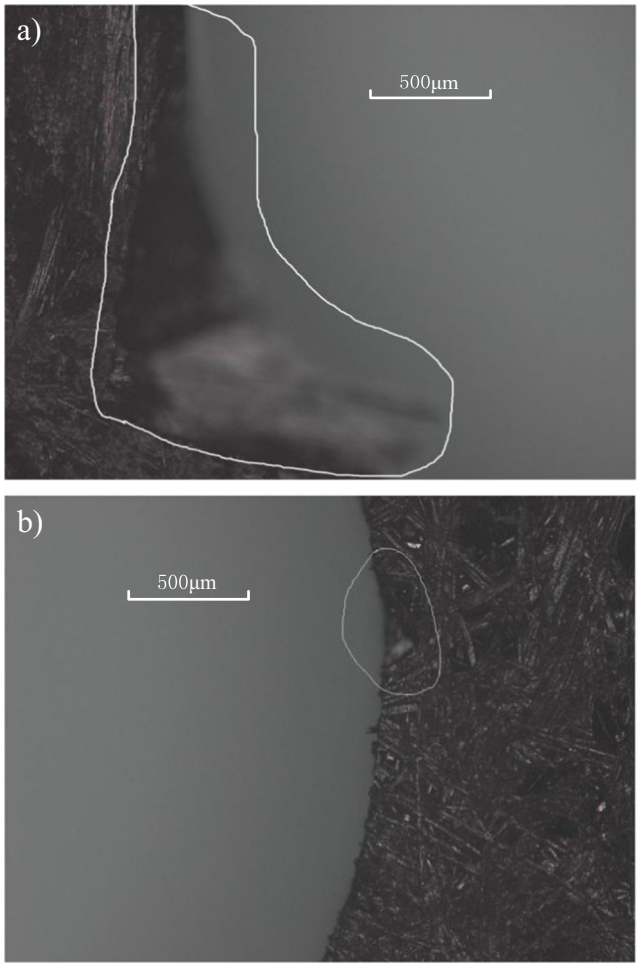

Fig. 19 Tear defects at the exit of the holes in RUD and CTD (n = 5000 rpm, F = 90mmpm). **a** RUD, **b** CTD

Tear factors in all the three types of drilling methods increase with the increasing of feed speed. However, the tendency of increasing in RUD is the slowest in all the three drilling methods.

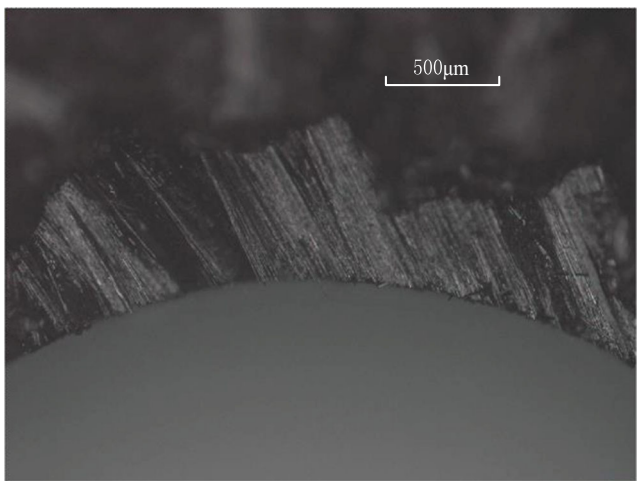

Fig. 20 Tears defects at the exit of the hole in HSD (n = 11,200 rpm, F = 90 mmpm)

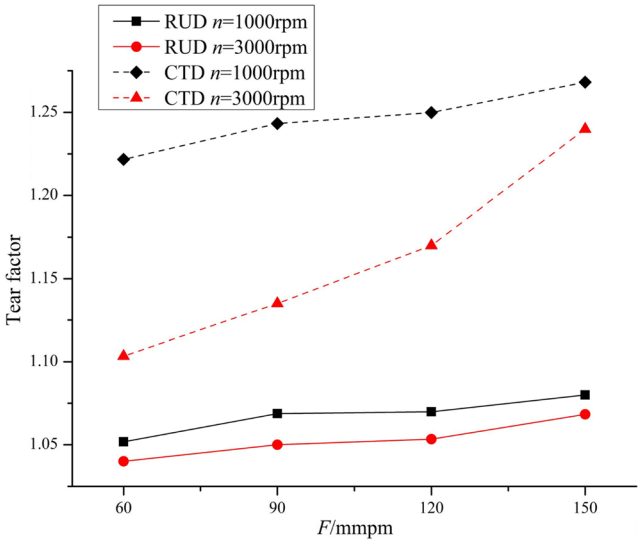

Fig. 21 Tear factors versus feed speed in RUD and CTD

Figure 22 shows that there is a fluctuation in the line graph of tear factors both in CTD and RUD, and the fluctuation in CTD is much greater than that in RUD. The tear factors in RUD and CTD show a gradually downward trend when the spindle speed increases from 1000 to 4000 rpm. However, they show a rise trend once the spindle speed exceeds 4000 rpm.

Figure 23 shows that the fluctuation in the line graph of tear factors in HSD is also much greater than that in RUD when the feed speed is greater than 120 mmpm and the spindle speed is greater than 7000 rpm. The situations of tear defects in HSD are more and more serious with the increasing of spindle speed and feed speed. Furthermore, most of the tear factors in HSD are more than 1.25 when the spindle speed reaches 14,000 rpm, which means these defects are delamination.

Therefore, the fluctuation of tear factors is consistent with the changes of drilling forces, and it also shows that drilling

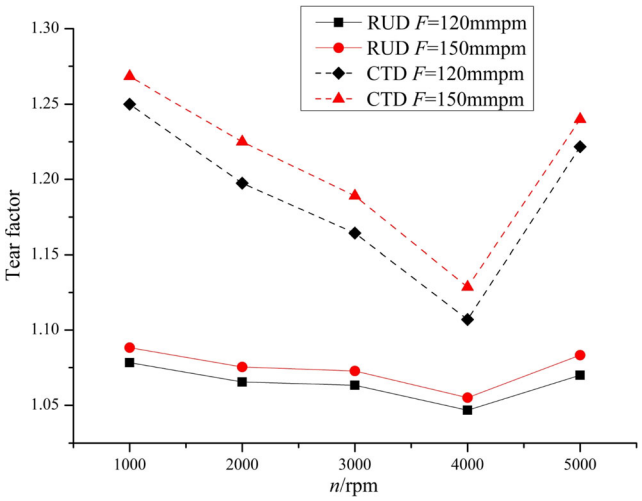

Fig. 22 Tear factors versus spindle speed in RUD and CTD

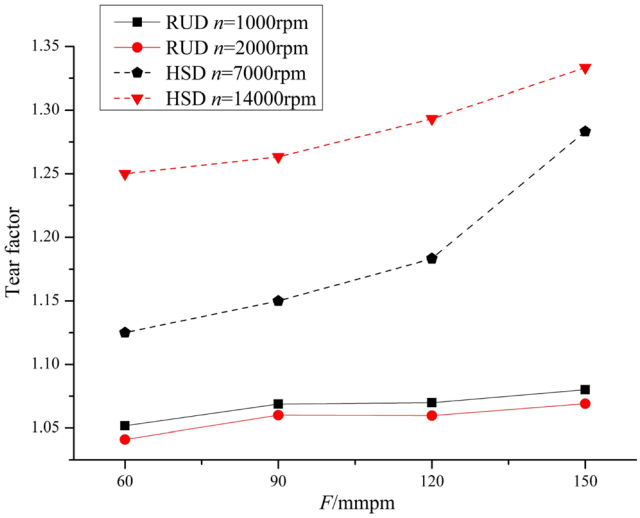

Fig. 23 Tear factors versus feed speed in RUD and HSD

forces have an important effect on drilling defects. If the drilling force becomes bigger and bigger, the defects will become more and more serious.

5 Conclusions

The effects of feed speed, cutting speed, and drilling method on hole quality, such as the defects of burr and tear, thrust force, and tool wear are analyzed during drilling of needle-punched C/C composites with K40 cemented carbide drill in this paper. Three types of drilling methods, including RUD, CTD, and HSD, are compared at the same feed speed. Based on the analysis of thrust force and drilling defects, the following conclusions can be drawn within the ranges of drilling parameters selected as follows:

1. Compared with CTD, thrust forces in RUD can be reduced greatly. Thrust forces in RUD are reduced by 41.9% at the greatest extent, and 26.5% at the average extent. Thrust forces can be reduced in HSD if the cutting speed is less than 24.49 m/min. However, thrust forces in HSD will increase quickly with the increasing of cutting speed once the cutting speed is greater than 24.49 m/min.
2. The effects of drilling parameters on thrust force are similar in RUD and CTD. However, the increasing speed of thrust forces in RUD is slower than that in CTD when feed speed and spindle speed increase.
3. Compared with CTD and HSD, RUD can effectively reduce tool wear and prolong tool life. Tool wear in HSD is the most serious of all due to its higher cutting temperature and thrust force.
4. At all levels of drilling parameters, tear factors in RUD are the smallest of all the three types of drilling methods. Although there are some improvements of decreasing burr defects in RUD, the effect is not obvious. HSD is conducive to cut off the fiber, thus burr defects can be reduced when feed speed is less than 120 mmpm and spindle speed is less than 9100 rpm. However, when feed speed is greater than 120 mmpm and spindle speed is greater than 9100 rpm, burr defects will increase slightly.
5. The effects of drilling parameters on tear factors are similar for the three types of drilling methods. However, the fluctuation of tear factors in RUD is the smallest of all. Hence, if the high cutting speed is used in RUD, the drilling defects may be reduced greatly before the tool wear becomes serious.

Funding Information This work is supported by "the National Natural Science Foundation of China" (No. 51105312) and "the Fundamental Research Funds for the Central Universities (No. 3102017gx06007)".

References

1. Savage E (2012) Carbon-carbon composites. Springer Science & Business Media
2. Buckley J (1988) Carbon-carbon-an overview
3. Kim D, Ramulu M (2004) Drilling process optimization for graphite/bismaleimide–titanium alloy stacks. Compos Struct 63(1):101–114. https://doi.org/10.1016/S0263-8223(03)00137-5
4. Cong W, Pei Z, Deines T, Liu D, Treadwell C (2013) Rotary ultrasonic machining of CFRP/Ti stacks using variable feedrate. Compos Part B 52:303–310. https://doi.org/10.1016/j.compositesb.2013.04.022
5. Debnath K, Singh I, Dvivedi A (2014) Rotary mode ultrasonic drilling of glass fiber-reinforced epoxy laminates. J Compos Mater 49(8):949–963. https://doi.org/10.1177/0021998314527857
6. Yuan S, Zhang C, Amin M, Fan H, Liu M (2015) Development of a cutting force prediction model based on brittle fracture for carbon fiber reinforced polymers for rotary ultrasonic drilling. Int J Adv Manuf Technol 81(5–8):1223–1231
7. Ning F, Cong W, Pei Z, Treadwell C (2016) Rotary ultrasonic machining of CFRP: a comparison with grinding. Ultrasonics 66:125–132
8. Wang J, Feng P, Zhang J, Zhang C, Pei Z (2016) Modeling the dependency of edge chipping size on the material properties and cutting force for rotary ultrasonic drilling of brittle materials. Int J Mach Tools Manuf 101:18–27. https://doi.org/10.1016/j.ijmachtools.2015.10.005
9. Li Z, Jiao Y, Deines T, Pei Z, Treadwell C (2005) Rotary ultrasonic machining of ceramic matrix composites: feasibility study and designed experiments. Int J Mach Tools Manuf 45(12):1402–1411
10. Liu J, Baek D, Ko T (2014) Chipping minimization in drilling ceramic materials with rotary ultrasonic machining. Int J Adv Manuf Technol 72(9–12):1527–1535. https://doi.org/10.1007/s00170-014-5766-y
11. Ning F, Wang H, Cong W, Fernando P (2017) A mechanistic ultrasonic vibration amplitude model during rotary ultrasonic machining of CFRP composites. Ultrasonics 76:44–51. https://doi.org/10.1016/j.ultras.2016.12.012
12. Cong W, Pei Z, Feng Q, Deines T, Treadwell C (2012) Rotary ultrasonic machining of CFRP: a comparison with twist drilling. J Reinf Plast Compos 31(5):313–321
13. Cong W, Pei Z, Sun X, Zhang C (2014) Rotary ultrasonic machining of CFRP: a mechanistic predictive model for cutting force. Ultrasonics 54(2):663–675

14. Liu J, Zhang D, Qin L, Yan L (2012) Feasibility study of the rotary ultrasonic elliptical machining of carbon fiber reinforced plastics (CFRP). Int J Mach Tools Manuf 53(1):141–150. https://doi.org/10.1016/j.ijmachtools.2011.10.007
15. Campos Rubio J, Abrão A, Eustáquio Faria P, Correia A, Davim J (2008) Delamination in high speed drilling of carbon fiber reinforced plastic (CFRP). J Compos Mater 42(15):1523–1532. https://doi.org/10.1177/0021998308092205
16. Wang C, Cheng K, Rakowski R, Greenwood D, Wale J (2016) Comparative studies on the effect of pilot drillings with application to high-speed drilling of carbon fibre reinforced plastic (CFRP) composites. Int J Adv Manuf Technol 89(9–12):3243–3255. https://doi.org/10.1007/s00170-016-9268-y
17. Karnik S, Gaitonde V, Rubio J, Correia A, Abrão A, Davim J (2008) Delamination analysis in high speed drilling of carbon fiber reinforced plastics (CFRP) using artificial neural network model. Mater Des 29(9):1768–1776. https://doi.org/10.1016/j.matdes.2008.03.014
18. Campos Rubio J, Abrao A, Faria P, Correia A, Davim J (2008) Effects of high speed in the drilling of glass fibre reinforced plastic: evaluation of the delamination factor. Int J Mach Tools Manuf 48(6):715–720. https://doi.org/10.1016/j.ijmachtools.2007.10.015
19. Lin S, Chen I (1996) Drilling carbon fiber-reinforced composite material at high speed. Wear 194(1):156–162
20. Gaitonde V, Karnik S, Rubio J, Correia A, Abrao A, Davim J (2008) Analysis of parametric influence on delamination in high-speed drilling of carbon fiber reinforced plastic composites. J Mater Process Technol 203(1):431–438
21. Krishnaraj V, Prabukarthi A, Ramanathan A, Elanghovan N, Senthil Kumar M, Zitoune R, Davim J (2012) Optimization of machining parameters at high speed drilling of carbon fiber reinforced plastic (CFRP) laminates. Compos Part B 43(4):1791–1799. https://doi.org/10.1016/j.compositesb.2012.01.007
22. Shan C, Wang X, Yang X, Lyu X (2015) Prediction of cutting forces in ball-end milling of 2.5 DC/C composites. Chin J Aeronaut 29(3):824–830
23. Shan C, Lin X, Wang X, Yan J, Cui D (2015) Defect analysis in drilling needle-punched carbon-carbon composites perpendicular to nonwoven fabrics. Adv Mech Eng 7(8):1–11. https://doi.org/10.1177/1687814015598494